AD-A038 069 WRIGHT STATE UNIV DAYTON OHIO DEPT OF ENGINEERING F/G 11/6
LIFE PREDICTION TECHNIQUES FOR ANALYZING CREEP-FATIGUE INTERACT--ETC(U)
NOV 76 M N MENON F33615-76-C-5030
UNCLASSIFIED AFML-TR-76-172 NL

1 OF 1
ADA038069

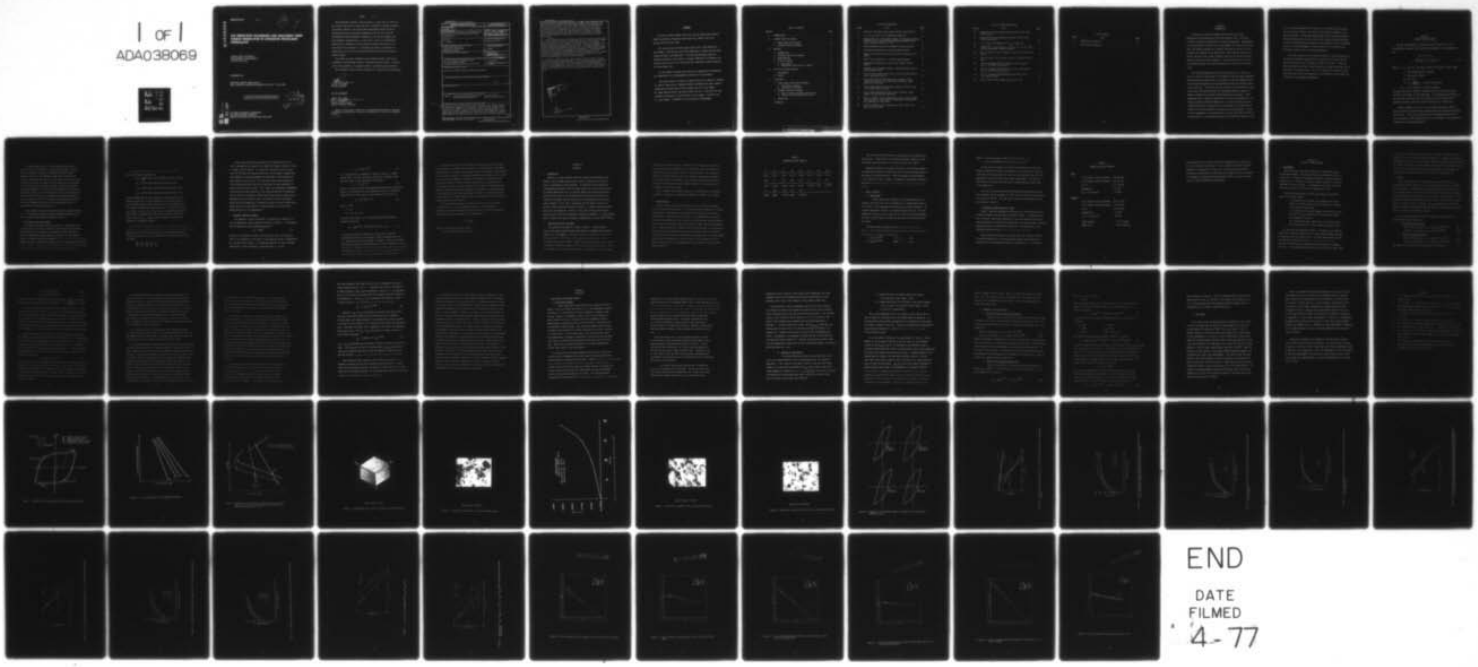

END
DATE FILMED
4-77

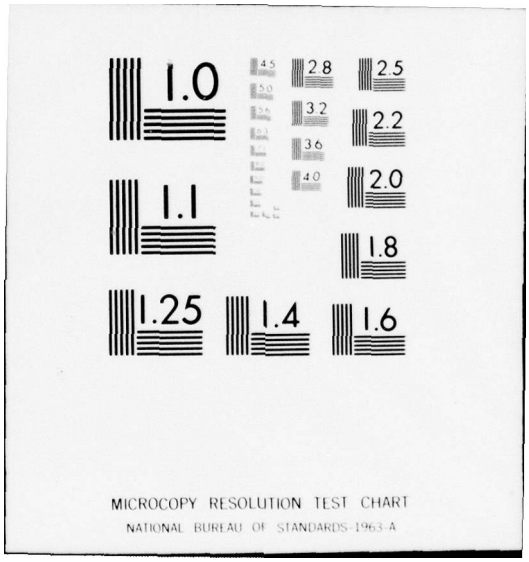
1.0
1.1
1.25
1.4
1.6
1.8
2.0
2.2
2.5
2.8
3.2
3.6
4.0
4.5
5.0
MICROCOPY RESOLUTION TEST CHART
NATIONAL BUREAU OF STANDARDS-1963-A

AFML-TR-76-172

LIFE PREDICTION TECHNIQUES FOR ANALYZING CREEP-FATIGUE INTERACTION IN ADVANCED NICKEL-BASE SUPERALLOYS

WRIGHT STATE UNIVERSITY
DEPARTMENT OF ENGINEERING
DAYTON, OHIO 45431

NOVEMBER 1976

TECHNICAL REPORT AFML-TR-76-172
FINAL TECHNICAL REPORT FOR PERIOD 8 JULY 1975 - 7 JULY 1976

AIR FORCE MATERIALS LABORATORY
AIR FORCE SYSTEMS COMMAND
WRIGHT-PATTERSON AIR FORCE BASE, OHIO 45433

NOTICE

When government drawings, specifications, or other data are used for any purpose other than in connection with a definitely related government procurement operation, the United States Government thereby incurs no responsibility nor any obligation whatsoever; and the fact that the government may have formulated, furnished, or in any way supplied the said drawings, specifications, or other data, is not to be regarded by implication or otherwise as in any manner licensing the holder or any other person or corporation, or conveying any rights or permission to manufacture, use, or sell any patented invention that may in any way be related thereto.

This report has been reviewed by the Information Office (10) and is releasable to the National Technical Information Service (NTIS). At NTIS, it will be available to the general public, including foreign nationals.

This technical report has been reviewed and is approved for publication.

WALTER H. REIMANN
Project Engineer

FOR THE COMMANDER

GAIL E. EICHELMAN
Metals Behavior Branch
Metals & Ceramics Division

Copies of this report should not be returned unless return is required by security consideration, contractual obligations, or notice on a specific document.

UNCLASSIFIED

SECURITY CLASSIFICATION OF THIS PAGE *(When Data Entered)*

REPORT DOCUMENTATION PAGE

READ INSTRUCTIONS BEFORE COMPLETING FORM

1. REPORT NUMBER: AFML-TR-76-172	2. GOVT ACCESSION NO.
3. RECIPIENT'S CATALOG NUMBER	
4. TITLE *(and Subtitle)*: Life Prediction Techniques for Analyzing Creep-Fatigue Interaction in Advanced Nickel-Base Superalloys	5. TYPE OF REPORT & PERIOD COVERED: Final Technical Report 08 July 75 to 07 July 76
	6. PERFORMING ORG. REPORT NUMBER
7. AUTHOR(s): M.N. Menon	8. CONTRACT OR GRANT NUMBER(s): F33615-76-C-5030
9. PERFORMING ORGANIZATION NAME AND ADDRESS: Wright State University, Department of Engineering, Dayton, Ohio 45431	10. PROGRAM ELEMENT, PROJECT, TASK AREA & WORK UNIT NUMBERS: 227901
11. CONTROLLING OFFICE NAME AND ADDRESS	12. REPORT DATE: November 1976
	13. NUMBER OF PAGES: 57
14. MONITORING AGENCY NAME & ADDRESS *(if different from Controlling Office)*: Air Force Materials Laboratory (LLN), Air Force Systems Command, Wright-Patterson Air Force Base, Ohio 45433	15. SECURITY CLASS. *(of this report)*: Unclassified
	15a. DECLASSIFICATION/DOWNGRADING SCHEDULE

16. DISTRIBUTION STATEMENT *(of this Report)*

Approved for public release; distribution unlimited.

17. DISTRIBUTION STATEMENT *(of the abstract entered in Block 20, if different from Report)*

409 559

18. SUPPLEMENTARY NOTES

19. KEY WORDS *(Continue on reverse side if necessary and identify by block number)*

RENE 95 Strain Range Partitioning Approach Low Cycle Fatigue
Frequency Modified Approach Creep-Fatigue Interaction

20. ABSTRACT *(Continue on reverse side if necessary and identify by block number)*

On the basis of the limited data that are presented in this study, it may be concluded that the effect of creep damage on the low cycle fatigue behavior of Rene 95 at 1200°F is not very severe. This is probably because of the good stress rupture properties of the material at this temperature. Strain Range Partitioning approach does not seem to hold much promise for analyzing, and therefore, for predicting strain controlled low cycle fatigue behavior

over

DD FORM 1 JAN 73 1473 EDITION OF 1 NOV 65 IS OBSOLETE

UNCLASSIFIED

SECURITY CLASSIFICATION OF THIS PAGE *(When Data Entered)*

of Rene 95 under creep-fatigue conditions at 1200°F. When compared to the SRP approach, the Frequency Modified approach appears less cumbersome and, hence, more advantageous. The present study indicates, however, that the FM approach using the frequencies calculated on the basis of the actual cycles holds only a slight edge over that involving unmodified inelastic strain range versus cyclic life representation. At present, the damage approach proposed by Ostergren seems to offer more potential as it takes into account the aspect of loop shift that accompanies fatigue cycling of Rene 95.

Most of the present data have been generated in the very low cycle range which may not be of interest to the designers who are concerned about fatigue lives representative of the conditions of actual service in an engine. Because Rene 95 is a high strength, low ductility alloy, the inelastic strain ranges encountered in fatigue cycling are small. It becomes difficult to measure them experimentally when the lives are in the range 10,000 to 50,000, not to mention any attempt at separation of components. In this regard, SRP approach is clearly at a disadvantage; FM approach based solely on the inelastic strain range, and the damage approach are probably less so. Between the latter two methods, FM approach is less sophisticated at it does not involve determination of the peak tensile stresses.

Therefore, considering life prediction from the point of view of total strain range (elastic plus inelastic) - cycles to failure behavior instead of elastic or inelastic strain range alone may be the best approach suited to Rene 95 at this temperature. Here, the FM approach is still applicable. As the field measurements of strain are in terms of total strain, total strain range - life representation is also more advantageous from a design point of view.

FOREWORD

The Final Technical Report covers all work performed under Contract F33615-76-C-5030 by the Wright State University, Dayton, Ohio from 08 July 1975 to 07 July 1976.

This contract was initiated under Project 2279, "Solid Mechanics", Task 227901, "Life Analysis and Failure Mechanisms in Engine and Airframe Structural Metals and Composites". The work was performed under the technical direction of Dr. Walter H. Reimann (AFML/LLN) of the Metals and Ceramics Division of the Air Force Materials Laboratory, Wright-Patterson Air Force Base, Ohio.

Dr. M.N. Menon of Wright State University, Department of Engineering, was responsible for the management and execution of the program.

The author wishes to express his appreciation to Dr. Walter H. Reimann, Lt. John M. Hyzak and Dr. Theodore Nicholas of AFML/LLN for their helpful suggestions and discussion of this research and to Dr. Joe Conway, Mr. James Berling and Mr. Ray Stenz of Mar Test Inc., Cincinnati for their valuable contribution to the execution of this program. The help from Lt. David Summer of AFML/DOC is also gratefully acknowledged.

TABLE OF CONTENTS

LIST OF ILLUSTRATIONS

LIST OF ILLUSTRATIONS (Cont'd)

LIST OF TABLES

SECTION I
INTRODUCTION

The design of recent jet engines entering USAF service has emphasized high performance and high thrust/weight ratios, resulting in higher stresses and temperatures on rotating components. Superimposed on the performance increases are new requirements for longer service life. Thus, the need has emerged for increased consideration of the low cycle fatigue (LCF) behavior of the engine disks, since the high stress cycles seen by the disks have in many instances made the LCF life the limiting design criterion for these components. Accurate prediction of LCF life has therefore become of increasing importance, for design of new engine disks.

The increased temperatures and stresses that a disk is likely to see as a result of these trends in the design of the jet engine components, has necessitated consideration of the problem of elevated temperature low cycle fatigue deformation and also deformation under the combined effects of LCF and creep. To meet the need for reliable life prediction that take into account the above mentioned time dependent mechanical behavior, a number of methods are currently being developed and evaluated. These approaches have in common an appreciation for the time dependency of the fatigue process at elevated temperatures. One area which has received increased attention in recent years in this regard is the prediction of service life of disk materials in advanced gas turbine engines. As the cost of replacement of the advanced disks is many times more than that of an older disk, it is extremely important that further work be done in the

area of elevated temperature LCF behavior of the advanced disk materials and to test the validity of the various life prediction methods in real engine situations. An improved understanding of the elevated temperature fatigue problem should not only lead to more reliable prediction methods, but also to improved design operating and environmental control procedures, as well as to the development of better materials to increase fatigue performance capabilities at elevated temperatures.

The primary objective of the present program was the establishment of the relevant parameters required for the application of the two current predictive models to the LCF behavior of Rene 95 at 1200°F. These two models have been receiving increased attention in recent years and will be discussed in the next section. Also it was hoped that the present study would elucidate further the mechanisms of LCF damage in Rene 95 under the influence of time dependent deformation.

SECTION II
CURRENT PREDICTIVE MODELS

The well known "Method of Universal Slopes"[1] predicts LCF life for completely reversed, strain-controlled conditions at low temperatures thus:

$$\Delta\varepsilon_t = \Delta\varepsilon_e + \Delta\varepsilon_{in}$$

$$\Delta\varepsilon_t = \frac{3.5\sigma_u}{E} N_f^{-0.12} + D^{0.6} N_f^{-0.6} \qquad (1)$$

where $\Delta\varepsilon_t$, $\Delta\varepsilon_e$ and $\Delta\varepsilon_{in}$ are total, elastic and inelastic strain ranges

σ_u = the ultimate tensile strength

E = the elastic modulus

N_f = LCF life

$D = \ln \left(\frac{100}{100-R.A.}\right)$, the tensile ductility

R.A. = the % reduction in area at fracture.

The power law shown in equation 1 between cycles-to-failure and plastic or total strain range is well established. The engineering significance of this law lies in the fact that the fatigue life can be predicted with engineering accuracy from the properties measured in a tensile test.

Initial attempts to use this law at elevated temperature showed in many cases that the prediction was unconservative when compared with actual test results. It was then recognized that time-dependent effects which are not present at room temperature have to be considered in the prediction techniques for elevated temperature.

In elevated temperature LCF, if the frequency of application of stress or strain is high enough to preclude any creep effect, life may still be predicted on the basis of the Method of Universal Slopes.[1] However, a reduction in the frequency of application of the stress or strain or introduction of a hold time in the tensile portion of the stress or strain cycle reduces the number of cycles needed to fail the specimen. This is because thermal activation can modify the deformation processes at elevated temperature. For example, plastic deformation can occur more readily and a number of diffusion controlled processes can be operative if sufficient time is allowed. Any life prediction method which forms the basis for prediction of service life under such conditions must incorporate the time dependent modification of the fatigue process, which is often termed the creep-fatigue interaction.

Two most notable approaches that have been gaining increased attention are: (1) Strain Range Partitioning Method (SRP method) by Manson et al.[2,3] and (2) Frequency Modified Method (FM method) by Coffin.[4]

1. STRAIN RANGE PARTITIONING APPROACH

This method, developed by Manson and co-workers is based on the concept that there are two forms of inelastic strain; plastic strain and creep strain which may exist separately or concurrently and that their interaction can influence the fracture behavior of materials to a considerable degree. An important feature of the method is that it draws a further distinction between the manner in which tensile inelastic strain is reversed by the compressive inelastic strain to establish a closed hysteresis loop. In the present form, therefore, this method is suited only for fully reversed cycling conditions.

As shown by the hysteresis loop in Figure 1, there are four basic strain reversal possibilities:

$\Delta\varepsilon_{pp}$: tensile plastic flow reversed by compressive plastic flow

$\Delta\varepsilon_{cc}$: tensile creep reversed by compressive creep

$\Delta\varepsilon_{pc}$: tensile plastic flow reversed by compressive creep

$\Delta\varepsilon_{cp}$: tensile creep reversed by compressive plastic flow

Having recognized the four basic components of strain that must be considered, the next step is to devise separate tests in which the major strain component would be one of these basic types, and to determine the life relations associated with each one of them, i.e., relations such as $\Delta\varepsilon_{pp}$ vs N_{pp}; $\Delta\varepsilon_{cc}$ vs N_{cc}, $\Delta\varepsilon_{cp}$ vs N_{cp} and $\Delta\varepsilon_{pc}$ vs N_{pc} where N_{ij} represents the life that is characteristic of the cycling loading in which the inelastic strain was $\Delta\varepsilon_{ij}$. Figure 2 shows a schematic of possible relationships in a hypothetical material.

As has been noted, any general loading cycle is considered to be made up of these four basic types by establishing the fraction of the total inelastic strain range, f_{ij}, for each, the expected life, N_f, can be computed by noting the life N_{ij} from the basic $\Delta\varepsilon_{ij}$ vs N_{ij} relations for each strain range and using the relation:

$$\frac{f_{pp}}{N_{pp}} + \frac{f_{pc}}{N_{pc}} + \frac{f_{cp}}{N_{cp}} + \frac{f_{cc}}{N_{cc}} = \frac{1}{N_f} \qquad (2)$$

Strain range partitioning approach which recognizes that cyclic life is governed by the capacity of a material to absorb inelastic strain is indeed a useful concept. In isothermal, continuous strain cycling lives for the Type 316 stainless steel over a wide range of temperatures and frequencies, the above approach has been able to provide upper and lower bounds on cyclic lives.[3] Also the partitioned strain range-cyclic life relationships were found to be insensitive to test temperature to within a factor of two on cyclic life. Where such temperature independent correlations have been obtained, it has been observed that the monotonic tensile (plastic) and rupture (creep) ductilities are also insensitive to temperature within a factor of two. Variation of tensile and rupture ductilities with temperature is believed to affect the partitioned strain range-cyclic life relationships in the same manner as in the Coffin-Manson equation for low temperatures.[3]

2. FREQUENCY MODIFIED APPROACH

This approach is due to Coffin[4] and is essentially an extension of the low temperature fatigue equation of Manson and Coffin. In the Manson-Coffin approach the basic governing equation is

$$\Delta\varepsilon_{in} = C_1 N_f^{-\beta} \qquad (3)$$

where N_f is the number of cycles to failure and β and C_1 are constants. There is no frequency or time factor in the equation, which is appropriate for low temperature fatigue. To extend the equation for use at elevated temperatures, Coffin introduced a frequency term, ν, to give

$$\Delta\varepsilon_{in} = C_2 \left(N_f \nu^{K-1}\right)^{-\beta} \tag{4}$$

K is a constant and C_2 is regarded as a measure of ductility. Another equation that is similarly modified for the effect of frequency relates the stress range, $\Delta\sigma$, and the inelastic strain range

$$\Delta\sigma = A \, \Delta\varepsilon_{in}^{n'} \nu^{K_1} \tag{5}$$

where A, n' and K_1 are coefficients determined from test data by regression analysis. Be eliminating $\Delta\varepsilon_{in}$ from equations (4) and (5), a relation between the elastic strain range, $\Delta\varepsilon_e$, and fatigue life, N_f, results in

$$\Delta\varepsilon_e = \frac{\Delta\sigma}{E} = \frac{A'}{E} N_f^{-\beta'} \nu^{K_1'} \tag{6}$$

where $A' = AC_2^{n'}$

$$\beta' = \beta n'$$

$$K_1' = -\beta n' (K-1) + K_1$$

The total strain range, $\Delta\varepsilon_t$, can be found analytically be combining equations (4) and (6)

$$\Delta\varepsilon_t = C_2(N_f\nu^{K-1})^{-\beta} + \frac{A}{E} C_2^{n'} N_f^{-\beta n'} \nu^{-\beta n'(K-1) + K_1} \tag{7}$$

The total strain range is considered to be the sum of an inelastic contribution and an elastic contribution. Material properties enter via C_2, a ductility value, and A, a measure of strength. K and K_1 are constants for a given situation which reflect the extent to which frequency is important. Introduction of frequency terms in the above fatigue equation in effect modifies the strength and ductility coefficients of the first equation proposed for completely reversed, strain-controlled conditions for low temperatures.

The general fatigue curve is idealized as being the sum of the two terms, each represented by straight lines in Figure 3. As stated earlier, increasing the temperature or decreasing the frequency shifts the "inelastic" curve and moves it to the left; the effect of increasing temperature on the elastic curve is less but the curve moves downwards. The point of intersection of the elastic and the inelastic curves is called transition fatigue life, N_T, which moves to a lower number of cycles. Coffin considers N_T to be critical in determining the method of testing and analytical procedures to be adopted. If the design life is less than N_T, LCF data and elastoplastic solutions are required for design; if the design life is higher than N_T, high cycle fatigue data and linear elastic stress analysis are more relevant.

Once the various constants are evaluated from LCF tests for different strain ranges and a set of frequencies, equation 7 can be employed to determine the LCF life under other sets of conditions. The hold time behavior can also be predicted from equation 7 by assuming that

$$\nu = \frac{1}{t_r + t_h}$$

where t_r is the time for strain reversal

t_h is the hold period for each cycle.

SECTION III

MATERIAL

1. INTRODUCTION

Rene 95 is a high strength nickel-base superalloy developed by the General Electric Company and primarily used for compressor and turbine disks in advanced gas turbine engines. In addition to the conventional strengthening mechanisms involving precipitation of a high volume fraction of ordered gamma-prime and, to a smaller degree solid solution hardening, Rene 95 derives part of its strength from the residual dislocation substructure introduced into the alloy during a thermomechanical processing (TMP) treatment. Also, TMP is responsible for the duplex structure of Rene 95, often called the "necklace structure", in which large warm worked grains are surrounded by a necklace of very small recrystallized grains. The net result of TMP and conventional hardening treatments is a large improvement in tensile and rupture strength at temperatures to about $1200^{o}F$ ($922^{o}K$).

2. PROCESSING AND HEAT TREATMENT

The composition of Rene 95 is given in Table 1. The processing starts with vacuum induction melted and vacuum arc remelted ingot, approximately 9 in. in diameter. This ingot is given a homogenization anneal in the range $2125^{o}F$ - $2175^{o}F$ for 3 hours and then furnace cooled. It is subsequently reheated to $2000^{o}F$ - $2080^{o}F$ and the primary processing reduction is applied to bring the thickness to 40 to 50% above the final value. This is followed by a recrystallization anneal at $2125^{o}F \pm 25^{o}F$ for an hour, which

results in a uniform grain size of ASTM 3-5. The forging is cooled from the recrystallization temperature at a rate greater than 150°F per hour to 1650°F and then air cooled or taken to final processing. The forging is reheated to 1975°F-2025°F and the final reduction is applied resulting in a 40 to 50% decrease in thickness. This imparts residual warm work into the material and allows the grain boundary regions to recrystallize into a necklace of very small grains.

Heat treatment after forging consists of a 2000°F partial solutioning treatment, oil quench to a temperature ≤900°F and a 1400°F, 16 hr. aging.

3. MICROSTRUCTURE

Figure 4 shows an optical micrograph of one of the Rene 95 pancakes with the necklace microstructure. The warm worked grains (WW) have a uniform distribution of intermediate-sized gamma prime precipitates, which give a darker shade to these grains in the optical. Surrounding the warm worked grains are the necklaces of very fine recrystallized grains, whose boundaries are decorated with overaged gamma prime that are larger than the intermediate-sized. Figure 5 shows the residual dislocation substructure in a warm worked grain which was introduced during the finish forging and which is anchored around and stabilized by the intermediate-sized gamma prime. The finest gamma prime which is responsible for the major part of the strength of Rene 95 appear as small spots in the background of the transmission electron micrograph (Figure 5).

TABLE 1

COMPOSITION OF RENE 95

C	Cr	Co	Fe	Mo	W	Ti	Al
0.15	13.8	8.0	0.13	3.50	3.57	2.50	3.55
Nb	B	Zr	Mn	Si	S	P	N
3.50	0.012	0.04	<0.10	<0.10	0.002	<0.01	0.003
O	Ag	Pb	Bi	Ni			
7ppm	<5ppm	<0.001	<1ppm	Balance			

The fine recrystallized grains of the necklace do not contain any substructure. Strewn mostly in the necklace regions, however, are the MC carbides which are high in Ti, Cb and W and low in Ni and Cr.

Observations made in the radial direction of the forging revealed no significant variation of either the size of the warm worked grains or the degree of recrystallization. Since the pancake was approximately 1 1/2 inches thick (and 15 inches in diameter), two specimens each were obtained through the thickness of the forging for tensile and fatigue testing.

4. TENSILE BEHAVIOR

A. Experimental

Tensile tests were conducted in an Instron machine using specimens that were 0.25 inch in diameter with a reduced gage length of 1.272 inches. The extensometer was attached to specimen shoulders. For elevated temperature testing, a resistance furnace was used. The room temperature test was run at a ramp rate of 0.05 inch per minute whereas, the tests at 1200°F were run using two ramp rates, 0.05 and 0.005 inch per minute.

The tensile data for Rene 95 at 75°F and 1200°F are given in Table 2. The following equations describe the flow stress versus strain relationships for monotonic deformation:

$$\sigma = 219.33(\varepsilon)^{0.022} \qquad 75°F \ldots\ldots\ldots\ldots (9)$$

$$\sigma = 240.94(\varepsilon)^{0.052} \qquad 1200°F \ldots\ldots\ldots\ldots (10)$$

where σ is the flow stress in KSI (engineering stress) and

ε is the corresponding strain (engineering strain).

At the low strain ranges, the strain-rate sensitivity of the flow stress at 1200°F was found to be negligible in that lowering of the ramp rate from 0.05 inch per minute to 0.005 inch per minute did not alter the magnitude of the flow stress versus strain relationship. The data for both rates of straining have been used for determining the coefficients in the equation 10.

The stress rupture properties were measured using Arcweld Creep and Stress Rupture Testing equipment at 1200°F under an initial load equivalent to a stress of 150 KSI. The creep rate along with other measured values are reported in Figure 6.

B. Deformation Substructure at 1200°F

Figure 7 shows the deformation substructure in the warm worked grains of Rene 95 samples that were tensile tested at 1200°F. In examining these foils, the most significant observation, as has been reported previously,[5] was the absence of any intense slip bands that are commonly found in deformed superalloys that are conventionally processed. The accumulation of deformation substructure was generally uniform and homogeneous.

Figure 8 shows the process of stacking fault and microtwin formation in the warm worked grains of necklace Rene 95 under creep conditions in accordance with the mechanisms proposed by Leverant et.al.[6] In addition,

TABLE 2

TENSILE DATA OF RENE 95

$75^{o}F$

0.1% offset yield strength	:	189.06 KSI
0.2% offset yield strength	:	192.61 KSI
U.T.S.	:	237.20 KSI
Elongation	:	11.76%
R.A. at fracture	:	12.88%

$1200^{o}F$

0.1% offset yield strength	:	167.77 KSI
0.2% offset yield strength	:	173.34 KSI
U.T.S.	:	217.95 KSI
Elongation	:	13.10%
R.A. at fracture	:	14.96%
Gage length	:	1.272 inches
Ramp rate	:	0.05 inch/min.

the examination also revealed substructure accumulation by ordinary slip of $\frac{\alpha}{2}\langle 110\rangle$ pairs of dislocations. Thus, at 1200°F and 150 KSI, Rene 95 deforms by a combination of viscous slip of partial dislocations contributing to the formation of microtwins and stacking faults, and ordinary slip movement of perfect dislocations which results in a general accumulation of tensile deformation substructure.

SECTION IV
LOW CYCLE FATIGUE BEHAVIOR

1. EXPERIMENTAL

Low cycle fatigue tests were conducted using standard hour glass button-head specimens. The minimum section was heated by means of an induction coil. A diametral extensometer along with a computer developed by Mar-Test Inc., Cincinnati, was used to monitor and control the strains developed in low cycle fatigue. The computer was calibrated to provide the axial strain and to control by the computed axial strain.

The following three modes of testing were employed in generating data for the present program:

(1) Continuous cycling under total computed axial strain control for various total axial strain ranges at a frequency of 20 cycles per minute (cpm).

(2) Continuous cycling under computed inelastic axial strain control for various computed axial inelastic strain ranges at a frequency of 0.05 cpm.

(3) Cycling under total computed axial strain control with a hold at the peak tensile strain, compressive strain or both.

All the tests were conducted at 1200°F. A triangular cyclic mode was chosen for (1) and (2) whereby the strain varied linearly between two equal and opposite limits (zero mean strain). The same linear mode was used for the continuous cycling part of the tests with hold times in which the rate of straining in the continuous part corresponded to a frequency of 20 cpm. In the above mentioned classification, total strain range refers

to the sum of the elastic and the inelastic components. The three modes of fatigue cycling are further illustrated in Figure 9. Although the diametral extensometry used in the present testing limited the highest frequency at which the closed loop hydraulic testing machine could be used for fatigue cycling to 20 cpm, this is believed to be a high enough frequency for precluding all time dependent deformation in Rene 95 at 1200°F, as discussed below.

2. RESULTS

Figure 10 shows the plot of the strain range versus cyclic life to failure relationships obtained for the 20 cpm and 0.05 cpm tests at 1200°F. AT 20 cpm, there is negligible time dependent deformation introduced in low cycle fatigue because of the high rate of straining. This is also evidenced by the appearance in these tests of Stage I type of crack initiation. Consequently, the inelastic strain range ($\Delta\varepsilon_{in}$) versus cyclic life (N_F) relationship at 20 cpm will also be referred to as $\Delta\varepsilon_{pp}$ versus N_{pp}, in accordance with the definition following the SRP approach, and can be modeled along the lines of classical Coffin-Manson equation.

The following equations describe the different strain range life relationships shown in Figure 10.

20 cpm Continuous Cycling

$$\text{Elastic strain range, } \Delta\varepsilon_e = 2.7240 \times 10^{-2} N_f^{-0.116} \quad (9)$$

$$\text{Inelastic strain range, } \Delta\varepsilon_{in} = 1.3874 N_f^{-0.998} \quad (10)$$

0.05 cpm Continuous Cycling

$$\text{Elastic strain range, } \Delta\varepsilon_e = 2.4289 \times 10^{-2} N_f^{-0.113} \quad (11)$$

$$\text{Inelastic strain range, } \Delta\varepsilon_{in} = 8.6557 \times 10^{-2} N_f^{-0.641} \quad (12)$$

The equations describing 20 cpm cycling may be rewritten as:

$$\Delta\varepsilon_e = 3.1745 \frac{\sigma u}{E} N_f^{-0.116} \quad (13)$$

$$\Delta\varepsilon_{in} = 8.5642 \, D \, N_f^{-0.998} \quad (14)$$

where σu, E and D are respectively the ultimate tensile strength the Young's modulus and the tensile ductility (as defined by $D = \ln \left(\frac{100}{100\text{-R.A.}}\right)$) at $1200^{o}F$.

The above equations were obtained by linear regression of the $\Delta\varepsilon$-N_f data on log-log coordinates. Based on $\Delta\varepsilon_{in}$-N_f plot, the equations predict higher lives at 0.05 cpm than at 20 cpm for low strain ranges. This prediction could not be tested out in the present program, as the inelastic strains are very difficult to control at such low values during testing. Also the times involved would have been too long. It must be noted that the above prediction is based on the assumption of a linear relationship, and more importantly on limited data.

Figure 11 shows the plot of the peak tensile and compressive stresses at $\frac{N_f}{2}$ developed in fatigue cycling of Rene 95 at $1200^{o}F$ and 20 cpm. The compressive stress is found to be approximately 10 ksi higher than the tensile stress. This difference is generally attributed to the increased true strain the material will be subjected to in compression, when cycled between two equal and opposite nominal strain limits. On a log-log plot, the best fit for σ_t versus $\Delta\varepsilon_{in}$ for 20 cpm tests would give:

$$\sigma_t = 339.86 \, (\Delta\varepsilon_{in})^{0.1254} \quad (15)$$

Figures 12 and 13 depict the change in the peak tensile and compressive stresses respectively of the hysteresis loop at half life as the frequency of cycling is lowered to 0.05 cpm from 20 cpm. Whereas the tensile stress drops with decrease in frequency, the compressive stress is found to remain unchanged. Even for the tensile part, the drop in stress is not large in view of the magnitude of the change in frequency.

The relationships between the inelastic strain range (measured at half life) and the cyclic life to failure obtained from hold-time tests involving symmetrical holds (i.e., equal hold times at both peak tensile and compressive strains) are presented in Figure 14. Also shown in the figure are the $\Delta\varepsilon_{in}$ vs N_f relationships for 0.05 cpm and 20 cpm continuous cycling tests. It is interesting to note that the 10/10 hold (i.e. 10 minutes in tension and 10 minutes in compression) was not any more damaging than the 1/1 hold in the higher strain ranges, when compared on the basis of the $\Delta\varepsilon_{in}$ vs N_f type of relationship. Consequently, only 1/1 hold tests were employed in determining the strain-life relationships at lower strain ranges.

The variation of cyclic life with inelastic strain range under unequal hold-time conditions is shown in Figure 15. The compressive holds are seen to be more damaging, than the tensile holds. Also shown is the line for the equal hold period tests which falls in between the 1/0 and the 0/1 hold lines.

An interesting observation involving the hold time tests is that the hysteresis loop shifts along the stress axis when unequal times were introduced. Figures 16 and 17 compare the shifts in peak tensile and compressive stresses respectively in reference to the peak values observed in 20 cpm and 0.05 cpm tests. The 0/1 type of hold tests shifts the peak tensile stress to a higher value (magnitude) while lowering the peak compressive stress thus displacing the whole hysteresis loop towards a mean stress value that offsets the mean compressive stress associated with the 20 cpm tests, with the result that an absolute mean tensile stress is produced. The reverse is found to be true for the 1/0 type of hold tests, in which the mean stress for the hysteresis loop is even more compressive than what is found in the 20 cpm tests. It is also interesting to note that for not too large inelastic strain ranges, 0/1 hold tests are associated with lower lives than

that observed for 1/0 type of hold tests (Figure 15). In addition, the 0/1 and the 1/0 lines are also found to cross near a N_f value of 100, indicating that at lives lower than 100 cycles (or equivalently at inelastic strain ranges greater than approximately 0.5 percent), the 1/0 hold would be more damaging to Rene 95 at 1200°F.

The observations of hysteresis loop shifts associated with unequal hold time tests in Rene 95 are similar to that found by Lord and Coffin[7] in fatigue cycling of Rene 80 with unequal hold times at 1600°F. In their study, tensile hold tests showed a compressive mean stress shift and the compressive hold tests showed a tensile mean stress shift. These shifts were explained in terms of the times spent in tensile and compressive loading. Qualitatively, the shorter lives found in the compressive hold tests could be explained on the basis of the increased tensile peak stress that the material would be subjected to and vice versa. It was also noted that the above mentioned behavior occurred in the life range above the transition fatigue life, which was taken to be an indicator of the mean stress capability of the material. From the present data, the transition fatigue life of Rene 95 at 1200°F is observed to be approximately 80 cycles (Figure 10), which is also close to the cross-over value of N_f for 0/1 and 1/0 hold test data (Figure 15).

From the above results, the partitioned strain range relationships were obtained in the following way. The data from the equal hold time tests were used to obtain the $\Delta\varepsilon_{cc}$ vs N_{cc} plot. The increment in the inelastic strain accompanying the hold at the peak strain was treated as a creep component, the remainder of the inelastic strain of the loop being then the plastic component. It was found that in equal hold tests,

the creep components (and hence also the plastic components) were equal in both compression and tension. Therefore, the inelastic deformation in these hysteresis loops could be analyzed in terms of cc + pp components. The N_{cc} life for each of the data point was computed using the interaction rule (Equation 2). The $\Delta\varepsilon_{cc}$ vs N_{cc} relationship thus derived is shown in Figure 18 and is best represented by the following equation:

$$\Delta\varepsilon_{cc} = 0.1375\ N_{cc}^{-0.806} \tag{16}$$

Similarly, $\Delta\varepsilon_{pc}$ vs N_{pc} relationship was derived from the 0/1 hold time data using the interaction rule involving pp and pc components. In these tests, the creep component in the compressive cycle was assumed to be equal to the increment in the inelastic strain during the compressive hold. That would also equal the pc component in the cycle, the remainder being the pp type. The $\Delta\varepsilon_{pc}$ vs N_{pc} relationship is shown in Figure 19 and follows the equation:

$$\Delta\varepsilon_{pc} = 8.2854 \times 10^{-2}\ N_{pc}^{-0.806} \tag{17}$$

$\Delta\varepsilon_{cp}$ vs N_{cp} relationship may be derived, likewise, from the 1/0 hold time tests. The triangles in Figure 19 represent the $\Delta\varepsilon_{cp}/N_{cp}$ points, which involve an inordinate amount of scatter as compared to that associated with the original $\Delta\varepsilon_{in}$-N_f results from which these points were derived.

Tests conducted under inelastic strain control at 0.05 cpm are also amenable to analysis by the strain range partitioning method. As these tests involve continuous cycling, the extent of creep strain that is introduced into the fatigue deformation is calculated using the drop in the peak stresses of the hysteresis loop as an indicator.

As discussed in Reference 3, when fatigue cycling is conducted at a high enough frequency to preclude all time dependent deformation, the corresponding hysteresis loops show the largest peak tensile or compressive stresses. During a continuous cycling test, when frequency is lowered from this high value, time dependent deformation sets in, which results in lowered peak stresses for the loops. For each frequency, a unique $\sigma_t(\sigma_c)$ versus $\Delta\varepsilon_{in}$ curve may be drawn. As the curve obtained at the highest frequency indicates the exact amount of time independent inelastic strain involved at a certain σ value, any excess inelastic strain observed for a test with the same σ value is believed to be the result of the time dependent deformation. For example, Figure 12 shows that decreasing the frequency from 20 cpm to 0.05 cpm lowers the peak tensile stress for the same inelastic strain range. In the absence of any differences in the mechanical behavior in the compressive and tensile directions, the same stress drop would be normally expected in the compressive peak stress also. However Rene 95 does exhibit a lower creep rate in the compressive direction, as a consequence of which, the σ_c vs $\Delta\varepsilon_{in}$ plot for 0.05 cpm shows very little shift from that for the 20 cpm plot (Figure 13). Following the manner in which the creep and plastic components are to be separated,[3] the 0.05 cpm hysteresis loops can be said to involve cp plus pp components rather than cc plus pp components which are normally expected. The cp points thus computed from the 0.05 cpm data are shown in Figure 19. The cp data were considered too scattered to obtain a representative relationship for a cp line in the form of an equation.

SECTION V
DISCUSSION

1. STRAIN RANGE PARTITIONING APPROACH

A. Some General Comments

Strain range partitioning approach which separates the total damage in low cycle fatigue into plastic (i.e., time independent inelastic) and creep (i.e., time dependent inelastic) components is indeed a useful concept. Generally, transgranular stage I type of crack initiation in smooth specimen cycling is associated with time independent inelastic damage whereas intergranular type of crack initiation is associated with time dependent inelastic damage. Any interaction between these two types of damage is then believed to influence the nature of the crack initiation in an actual test. In the present study, crack initiation lives, which were determined by the change in compliance of the test set-up, were found to be equal to or greater than 90 percent of the total cycles to failure (N_f). Hence, only N_f values were used for all the plots representing various strain range vs life relationships.

In fatigue cycling involving components other than pp, the most preferred cycle for introducing creep strain seems to be the one involving a constant tensile or compressive creep stress. However, this type of cycling could not be employed in the present study for two reasons. Firstly, during fatigue cycling of Rene 95 at equal and constant stresses, the average compressive creep rate was found to be approximately an order of magnitude smaller than the average creep rate in tension. This would have meant a prohibitively large amount of time for obtaining a given amount of compressive

creep strain if a value of tensile stress was used which would give the required tensile creep strain in a reasonable length of time. On the other hand, increasing the stress level in order to accelerate the compressive creep rate would have resulted in too short a time for tensile creep. One way to circumvent this problem would have been to bias the stress in the compressive direction. This method, however, was not followed, as it was found that the creep rates did not remain constant during continued cycling. In addition, the proportion of pp to cc strain was observed to change drastically during the course of fatigue cycling with a biased stress situation. Therefore, constant stress hold cycles were not employed; instead, constant strain hold cycles were used.

Rene 95 was found to be a cyclically softening material at 1200°F in that the stress range continuously decreased and the inelastic strain range continuously increased during the course of the test. This was true even for the 20 cpm cycling. As a result, the creep component in the hold time tests varied slightly during the tests. Therefore, stress or strain values at half the cyclic life was taken as representative of the hysteresis loop and were used in all the calculations and in determining the various life relationships.

All the test points, except two, were used in determining $\Delta\varepsilon_{ij}$ vs N_{ij} relationships for the SRP model. The two test points which could not be used were those corresponding to the 1 percent total strain range tests with unequal hold times (i.e., 1/0 and 0/1 hold tests).

Although the total inelastic strain range could be measured, the creep component could not be separated from the total value because of the extremely small value of the inelastic strain range to begin with.

The calculation of the cp components from 0.05 cpm tests involved first drawing a smooth curve through the tensile stress versus inelastic strain range data points from the 0.05 cpm and 20 cpm tests. For selected values of total inelastic strain ranges (0·1, 0·2, 0·3 and 0·4%), the tensile creep component was computed using the method described in Reference 3. At these same strain ranges, the $N_{observed}$ values were computed based on the best fit of all the five 0.05 cpm test points (i.e., equation 12). Equation 10 was used to calculate the corresponding N_{pp} values. Consequently, the computed cp points from the 0.05 cpm tests do not show much scatter (Figure 19). Had the individual test points rather than the smoothed-out values been used for calculations however, the scatter would have been much larger.

B. Validity of Test Points

A criterion that must be met for each test point to be used in the establishment of the life relationships was put forward in Reference 8. The criterion to be used is that at least one half of the damage ϕ in a test with an observed life N_{obs} must be due to the strain range component of interest (e.g., $\phi = F_{ij}\ (N_{obs}/N_{ij}) > 0.5$ for an ij cycle). An examination of the present data reveals that this criterion is met for all the test points except the following:

(i) Equal hold test (1/1 hold); total strain range = 1·2%; inelastic strain range = 0·12%.

(ii) Unequal hold tests (all 1/0 hold); total strain ranges = 1·8%, 1·4% and 1·2%; inelastic strain ranges = 0·52%, 0·3% and 0·21% respectively .

The cc point computed from (i) is, however, quite close to the cc line in Figure 18, and shows one of the lowest amount of deviation. On the other hand, the cp points computed from (ii) represent a large amount of scatter as shown in Figure 19. Instead of discounting the importance of these three test points, it is more beneficial to look at the basis of the criterion itself.

In all the tests, the value of F_{ij} was between 0·1 and 0·4. Hence, whether or not the above criterion is met for each test point depends largely on the N_{obs}/N_{ij} ratio. As mentioned in the previous section, 1/0 type of hold tests show a shift of the hysteresis loop in the compressive direction, thus lowering the peak tensile stress. Probably because of the lowered tensile stresses, for equivalent inelastic strains, 1/0 hold tests show lives close to those of the 20 cpm tests, the latter being the basis for the pp relationship. N_{obs}/N_{cp} ratio could then be expected to become smaller, which leads to the breakdown of the damage criterion. The loop shifts accompanying unequal hold tests seem to be a general phenomenon associated with fatigue cycling of high strength nickel base superalloys[7] and its importance in being able to influence the fatigue lives must not be discounted. Therefore, the present results reflect

upon the damage criterion itself, which is actually the basis for the SRP rule. It is felt that the use of the damage criterion and thus the SRP may have to be reevaluated from the point of view of its applicability to nickel base superalloys.

2. FREQUENCY MODIFIED APPROACH

A. Results without Frequency Modification

Figures 20 and 21 show all the test points when plotted in terms of inelastic and elastic strain ranges respectively versus cyclic life. The following equations represent the above relationships on the basis of a least squares fit:

$$\text{Inelastic strain range} = \Delta\varepsilon_{in} = 0.3147\ N_f^{-0.815} \tag{18}$$

$$\text{Elastic strain range} = \Delta\varepsilon_{e} = 2.0106 \times 10^{-2}\ N_f^{-0.082} \tag{19}$$

Figure 20 represents a difference of a factor of 8 between the extreme values in cyclic lives for a certain value of inelastic strain range. This difference is more than two orders of magnitude for the elastic strain range plot. On the basis of these results, a lower bound life for the conditions similar to those employed in this program may be estimated to be equal to $N_{f/3}$, where N_f is that life computed from the equation 18.

B. Results with Frequency Modification

Figure 22 represents the frequency modified relationship, in which $[\Delta\varepsilon_{in} \times (\frac{\nu}{20})^{-m}]$ is plotted versus N_f on log-log coordinates. It can be represented by the equation:

$$\Delta\varepsilon_{in} \times (\frac{\nu}{20})^{-0.10} = 0.6507\ N_f^{-0.882} \tag{20}$$

Here, $m = \beta (1-K) - -.10$ and

$\beta = 0.882$

The least square method gives an average K value for all the test points at 0.887. The frequency modified elastic plot is shown in Figure 23. It follows the equation

$$\Delta\varepsilon_e \times (\frac{\nu}{20})^{-0.03} = 2.5002 \times 10^{-2} (N_f)^{-0.103} \qquad (21)$$

The coefficients for the frequency modified approach are, therefore, the following:

$\beta = 0.882$ $\qquad$ $\beta' = 0.103$

$K = 0.887$ $\qquad$ $K_1' = 0.03$

$C_2 = 0.6507$ $\qquad$ $\frac{A'}{E} = 2.5002 \times 10^{-2}$

The complete frequency modified equation for Rene 95 at $1200^{o}F$ is

$$\Delta\varepsilon_t = 2.5002 \times 10^{-2} N_f^{-0.103} (\frac{\nu}{20})^{0.03} + 0.6507 N_f^{-0.882} (\frac{\nu}{20})^{0.10} \qquad (22)$$

Using the FM approach to model the inelastic strain range versus life data results in a scatter band of a factor of 7. This, however, can be further reduced to a factor of 4 if the data are plotted in the manner proposed by Ostergren,[9] in which the cyclic life is correlated with the tensile part of the hysterectic energy and which is frequency modified for the time dependent effects. The damage function proposed by Ostergren is given by

$$\sigma_t \times \Delta\varepsilon_{in} \times (\frac{\nu}{20})^{-m}$$

where σ_t is the peak tensile stress of the hysteresis loop at half life. The function represents an approximate value of the energy spent in the tensile part of the hysteresis loop. The relationship between the damage function and the cyclic life for Rene 95 is given by the equation:

$$\sigma_t \times \Delta\varepsilon_{in} \times (\frac{\nu}{20})^{-0.125} = 2.7212 \times 10^{2} N_f^{-1034} \qquad (23)$$

and is plotted in Figure 24. Figure 25 shows the plot of total strain range versus life for all the data. Also shown in this figure are $\Delta\varepsilon_t$ vs. N_f curves obtained from the frequency modified equation (23) for frequencies of 20, 0.95283, 0.4878 and 0.05 cpm.

3. CONCLUSIONS

On the basis of the limited data that are presented in this study, it may be concluded that the effect of creep damage on the low cycle fatigue behavior of Rene 95 at 1200°F is not very severe. This is probably because of the good stress rupture properties of the material at this temperature. As a result of this limited plastic flow, Strain Range Partitioning approach does not seem to hold much promise for analyzing, and, therefore, for predicting strain controlled low cycle fatigue behavior of Rene 95 under creep-fatigue conditions at 1200°F. When compared to the SRP approach, the Frequency Modified approach appears less cumbersome and, hence, more advantageous. The present study indicates, however, that the FM approach using the frequencies calculated on the basis of the actual cycles holds only a slight edge over that involving unmodified inelastic strain range versus cyclic life representation. At present, the damage approach proposed by Ostergren seems to offer more potential as it takes into account the aspect of loop shift that accompanies fatigue cycling of Rene 95.

Most of the present data have been generated in the very low cycle range which may not be of interest to the designers who are concerned about fatigue lives representative of the conditions of actual service in an engine. Because Rene 95 is a high strength, low ductility alloy, the inelastic strain ranges encountered in fatigue cycling are small. It becomes difficult to measure them experimentally when the lives are in the range 10,000 to 50,000, not to mention any attempt at separation of components. In this regard, SRP approach is clearly at a disadvantage; FM approach based solely on the inelastic strain range, and the damage apprcach are probably less so. Between the latter two methods, FM approach is less sophisticated as it does not involve determination of the peak tensile stresses.

Therefore, considering life prediction from the point of view of total strain range (elastic plus inelastic) - cycles to failure instead of elastic or inelastic strain range alone may be the best approach suited to Rene 95 at this temperature. Here, the FM approach is still applicable. As the field measurements of strain are in terms of total strain, total strain range-life representation is also more advantageous from a design point of view.

REFERENCES

1. S. S. Manson, Thermal Stress and Low Cycle Fatigue. McGraw-Hill Book Company, 1966.
2. S. S. Manson, G. R. Halford, and M. H. Hirschberg, "Creep Fatigue Analysis by Strain Range Partitioning", Symposium on Design for Elevated Temperature Environment, ASME, New York, 1971, pp 12-24.
3. S. S. Manson, Fatigue at Elevated Temperatures, ASTM-STP-520, 1973, pp 744-782.
4. L. F. Coffin, Jr., Fatigue at Elevated Temperatures, ibid, pp 5-34.
5. M. N. Menon, and W. H. Reimann, Metallurgical Transactions, 6A, 1975, 1075.
6. G. R. Leverant, and B. H. Kear, Metallurgical Transactions, 1, 1970, 491.
7. D. C. Lord, and L. F. Coffin, Jr., Metallurgical Transactions, 4, 1973, 1647.
8. M. H. Hirschberg, and G. R. Halford, NASA Technical Note, NASA TN D-8072, January 1976.
9. W. J. Ostergren, A Damage Function for Predicting Hold Time and Frequency Effects in Elevated Temperature Fatigue, Ph.D. Thesis work at Rensselaer Polytechnic Institute, 1974.

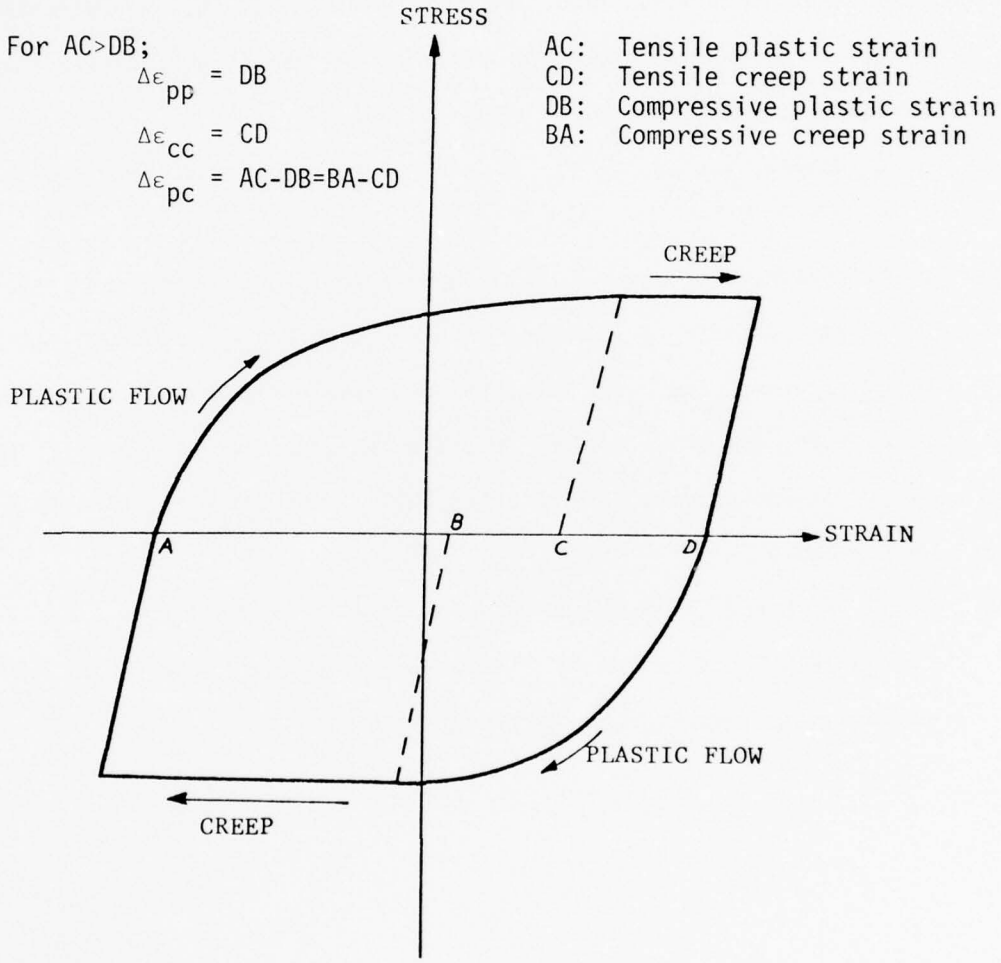

Figure 1. Hysteresis loop describing strain reversal possibilities.

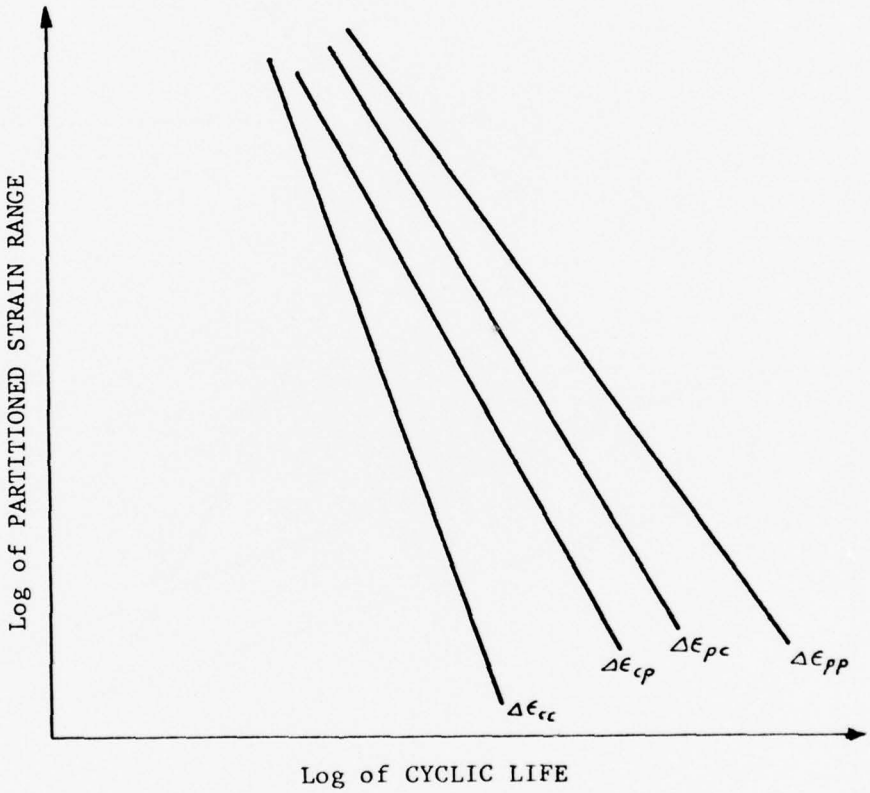

Figure 2. $\Delta\varepsilon_{ij}$ vs N_{ij} curves for a hypothetical material.

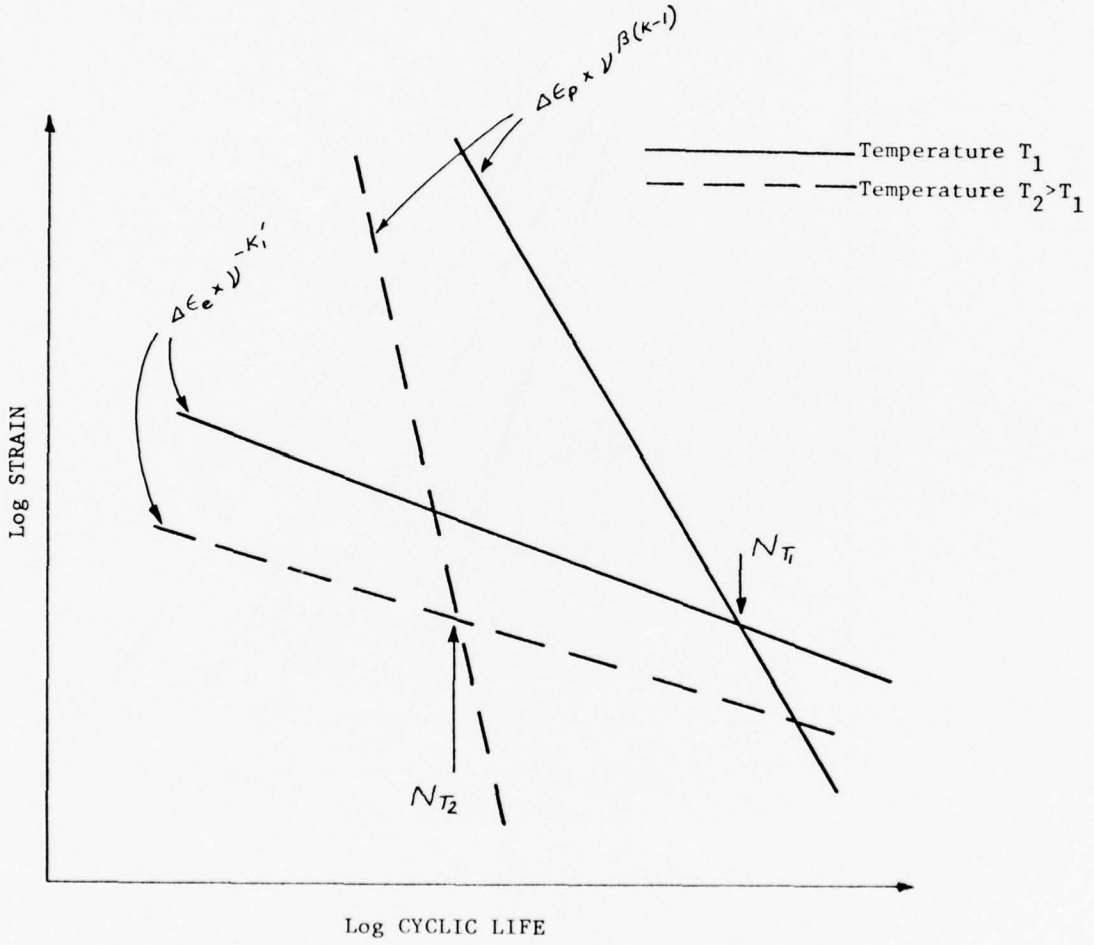

Figure 3. Representation of relationship between the frequency modified inelastic strain range, and the frequency modified elastic strain range and the cyclic life.

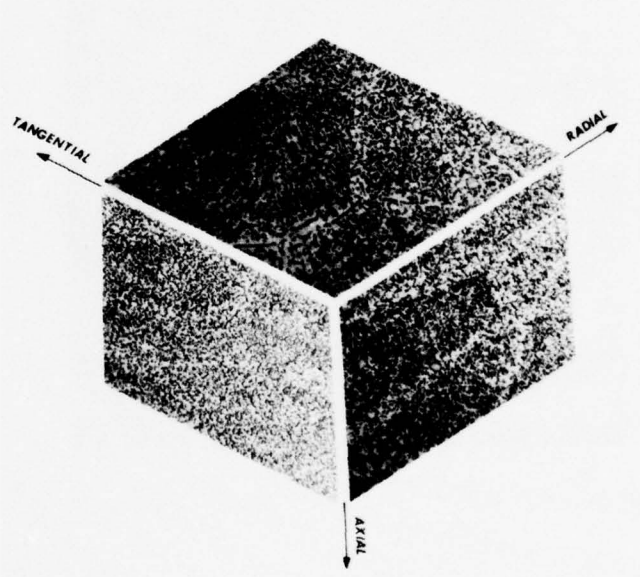

Magnification: 165 X

Figure 4. Three-dimensional optical micrograph of Rene 95 pancake.

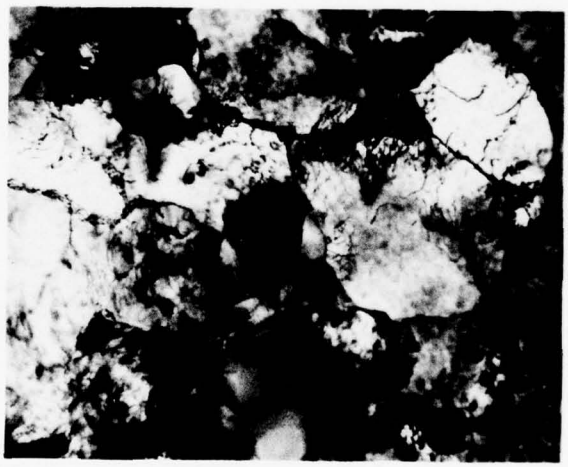

Magnification: 14000 X

Figure 5. Dislocation substructure in the warm worked grains.

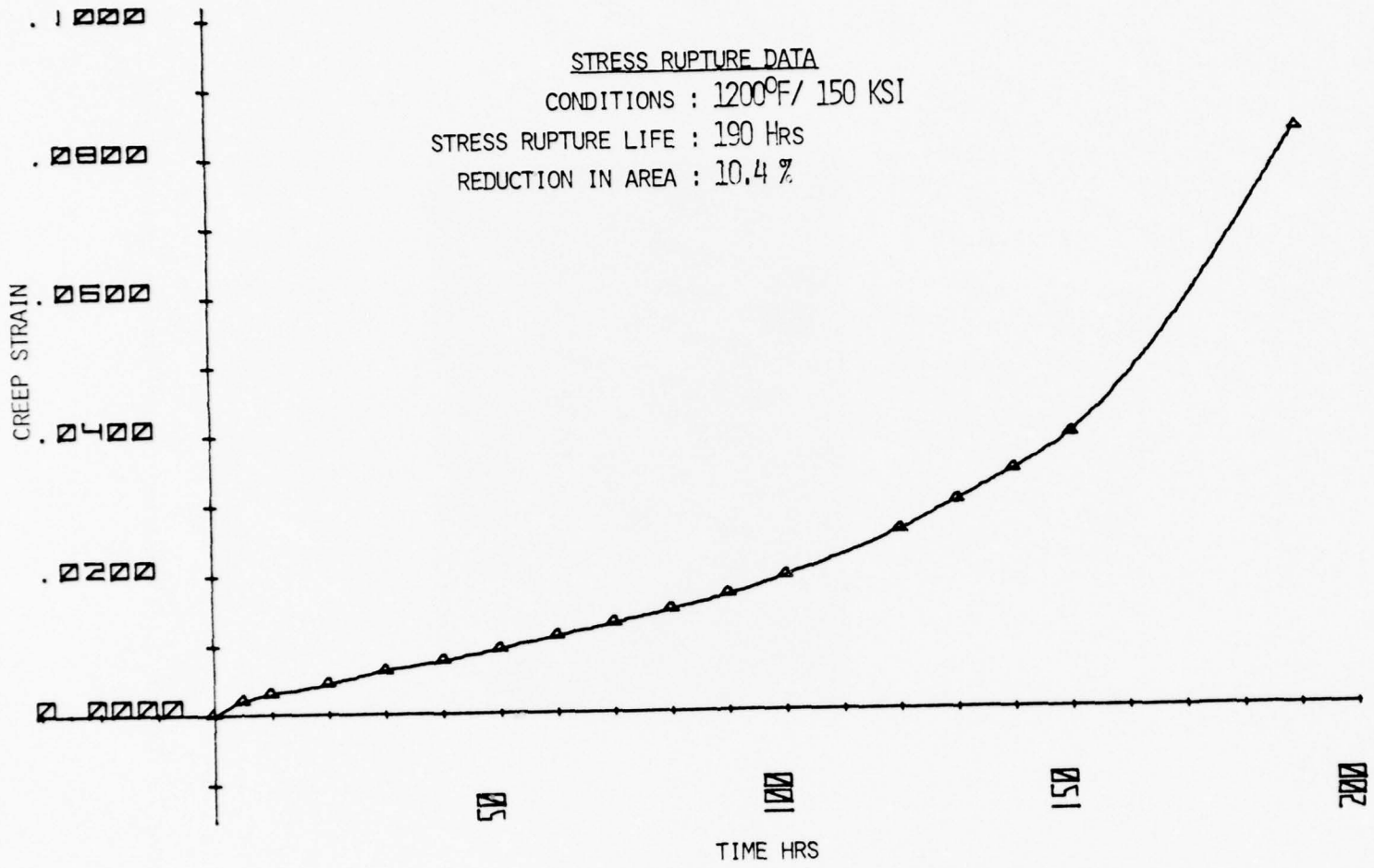

Figure 6. Plot of creep strain versus time in stress rupture test at 1200°F.

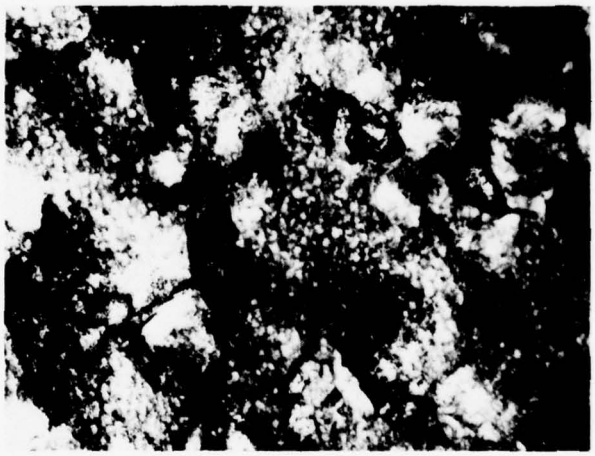

Magnification: 16500 X

Figure 7. TEM of foils prepared from a tensile-tested sample.

Magnification: 14000X

Figure 8. Deformation substructure from a stress rupture tested sample.

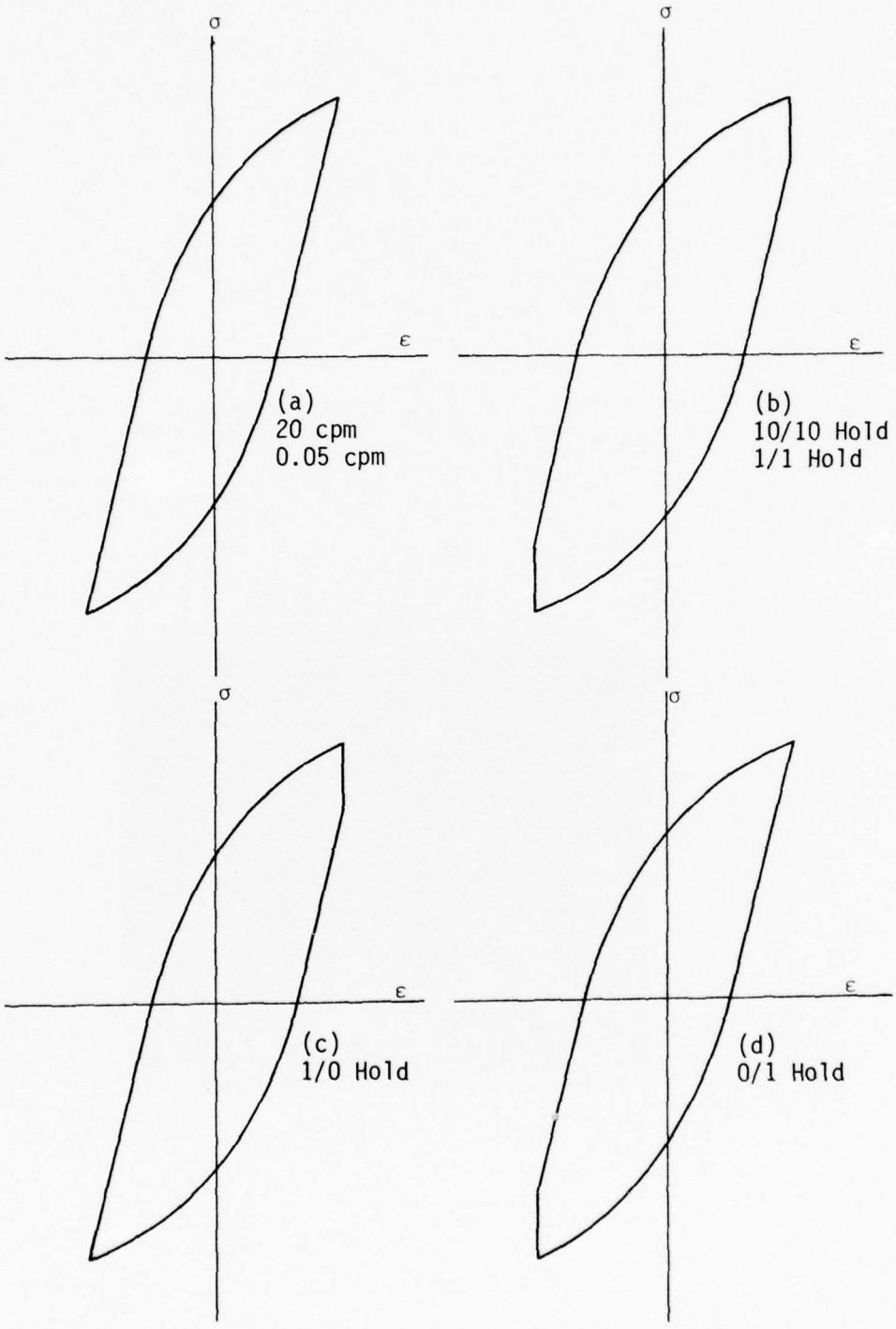

Figure 9. Examples of the different modes of fatigue cycling used in the isothermal tests.

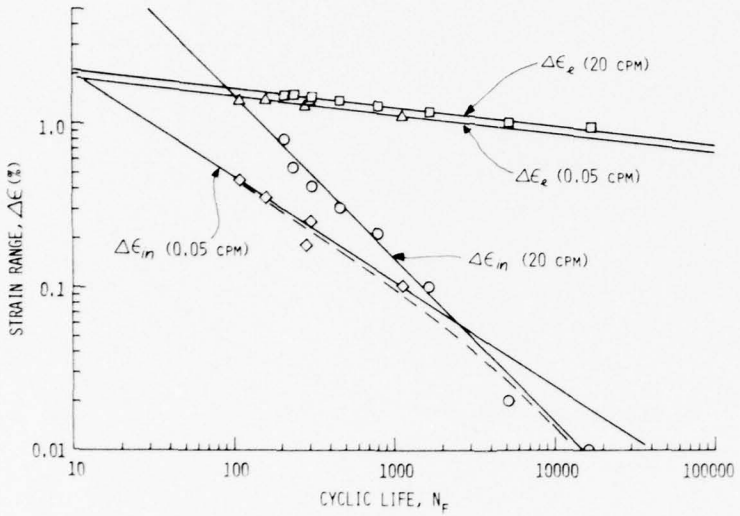

Figure 10. Plot of strain range versus cyclic life at 20 cpm and 0.05 cpm in continuous cycling.

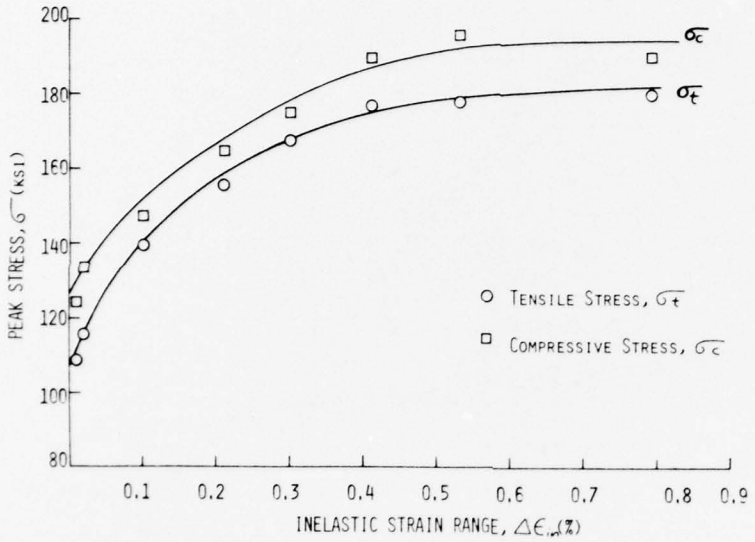

Figure 11. Plot of peak tensile and compressive stresses of the hysteresis loops at half lives versus inelastic strain range in 20 cpm tests.

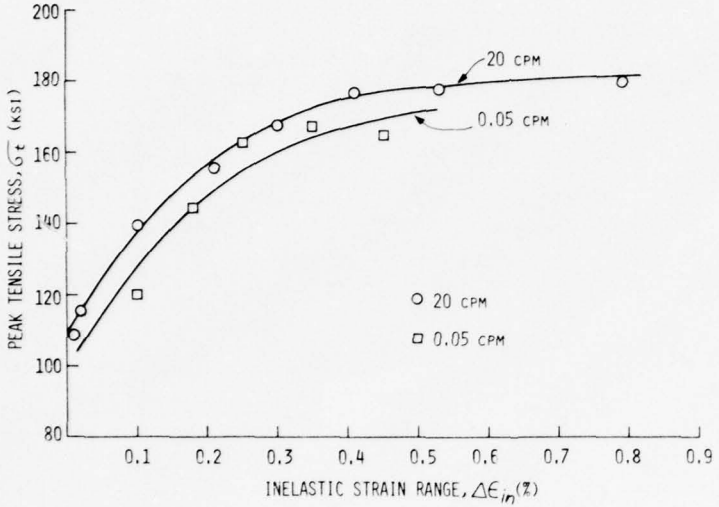

Figure 12. Plot of peak tensile stress versus inelastic strain range in 20 cpm and 0.05 cpm tests.

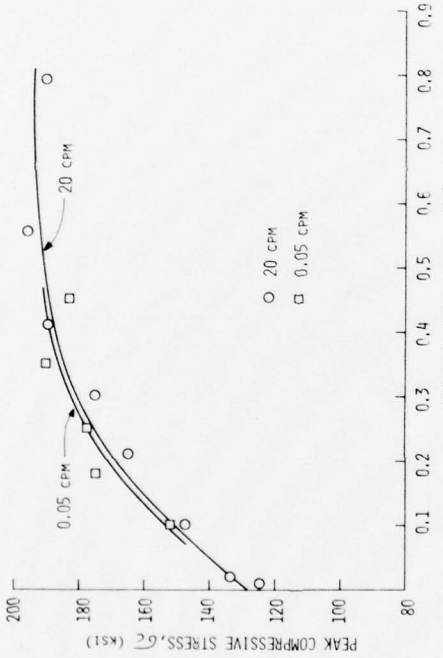

Figure 13. Plot of peak compressive stress versus inelastic strain range in 20 cpm and 0.05 cpm tests.

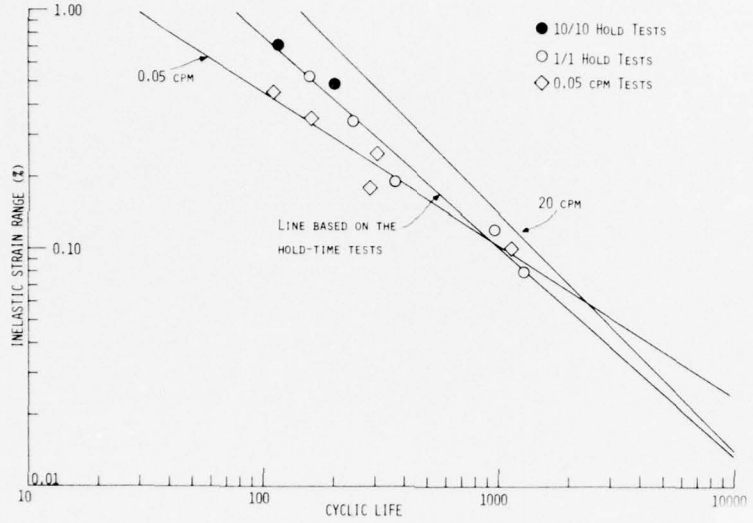

Figure 14. Plot of inelastic strain range versus cyclic life in equal hold time tests. Also shown are data points from the 0.05 cpm continuous cycling tests.

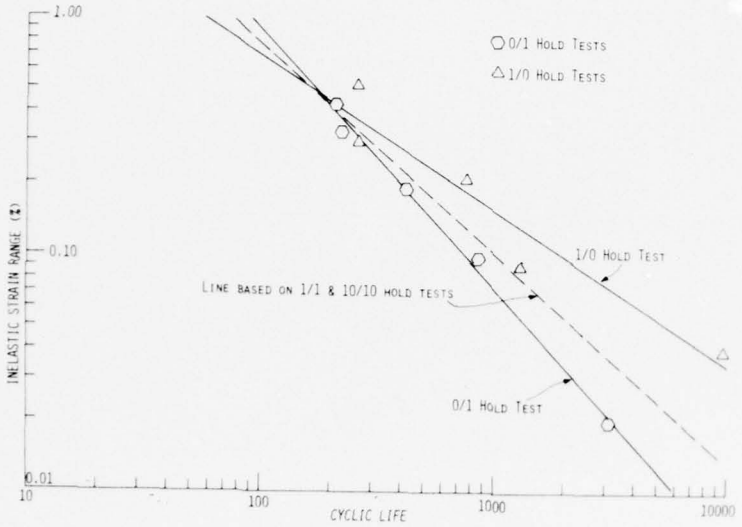

Figure 15. Plot of inelastic strain range versus cyclic life in unequal hold time tests.

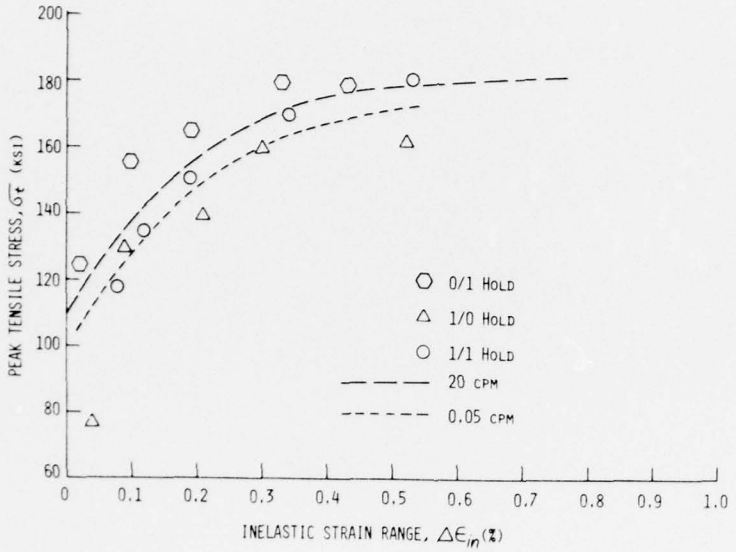

Figure 16. Comparison of peak tensile stresses at half lives from various tests.

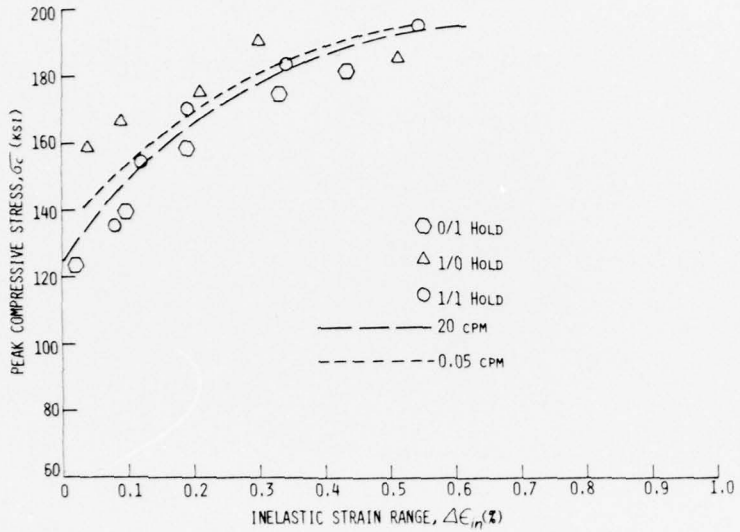

Figure 17. Comparison of peak compressive stresses at half lives from various tests.

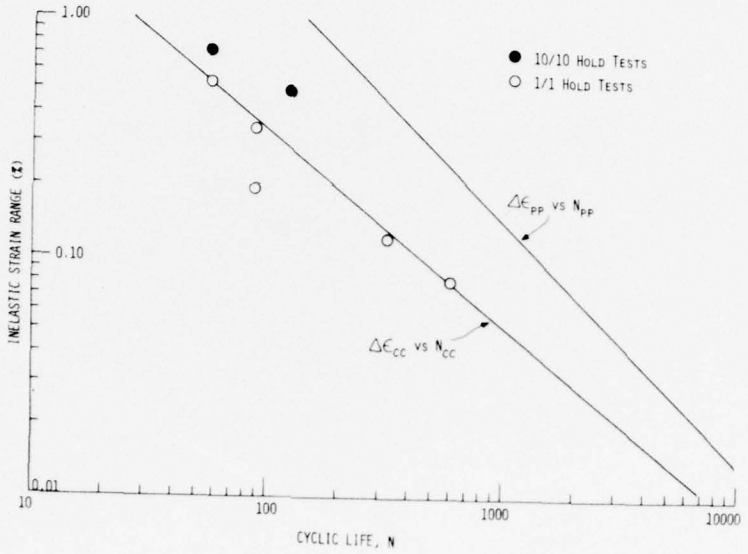

Figure 18. $\Delta\varepsilon_{cc}$ vs N_{cc} line compared with $\Delta\varepsilon_{pp}$ vs N_{pp} line.

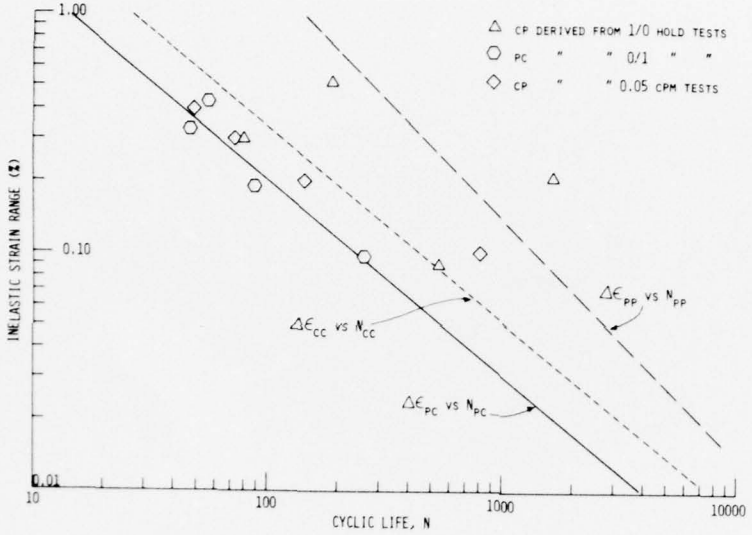

Figure 19. Comparison of $\Delta\varepsilon_{pp}$ vs N_{pp}, $\Delta\varepsilon_{cc}$ vs N_{cc}, $\Delta\varepsilon_{pc}$ vs N_{pc} plots and the data points from the cp tests.

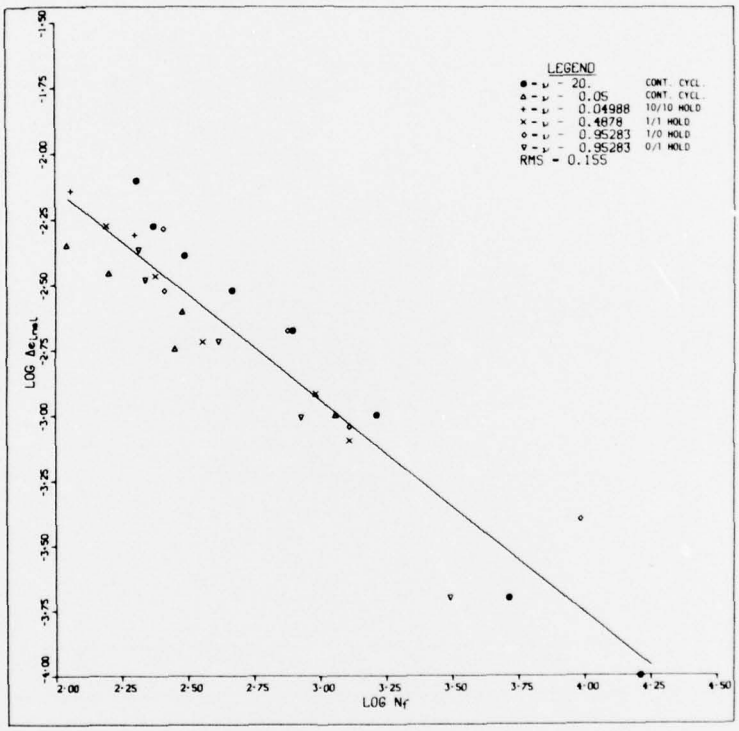

Figure 20. Plot of inelastic strain range vs cyclic life from all the tests.

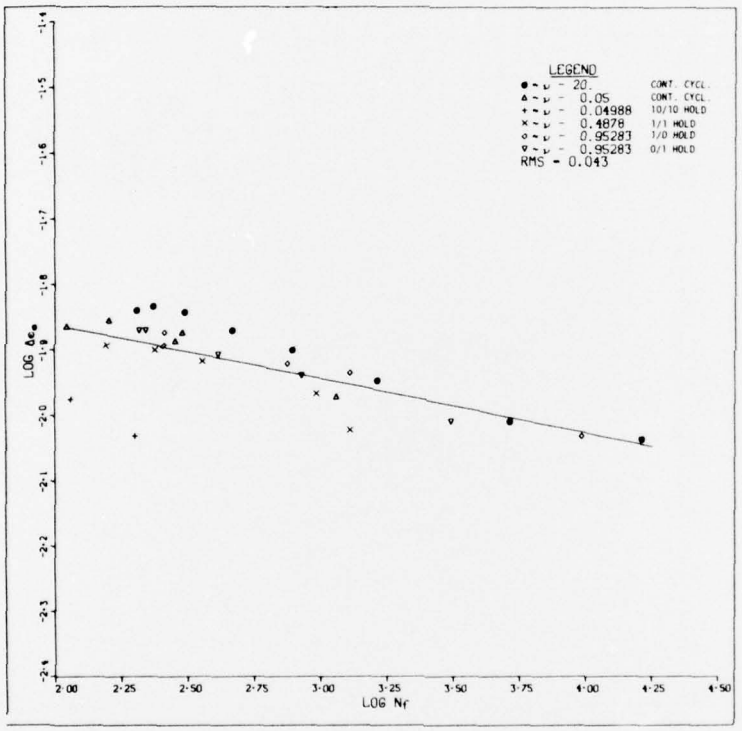

Figure 21. Plot of elastic strain range vs cyclic life from all the tests.

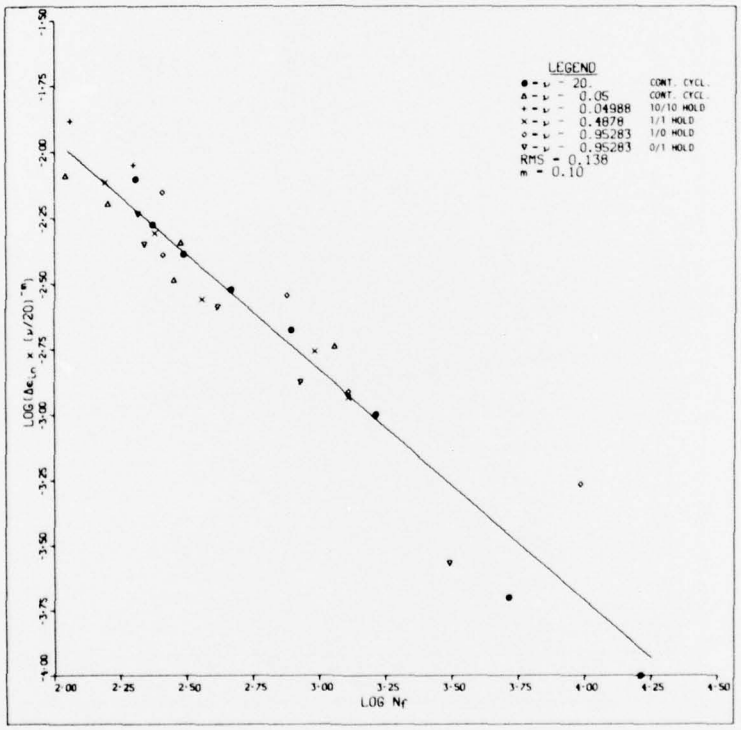

Figure 22. Plot of frequency modified inelastic strain range vs cyclic life from all the tests.

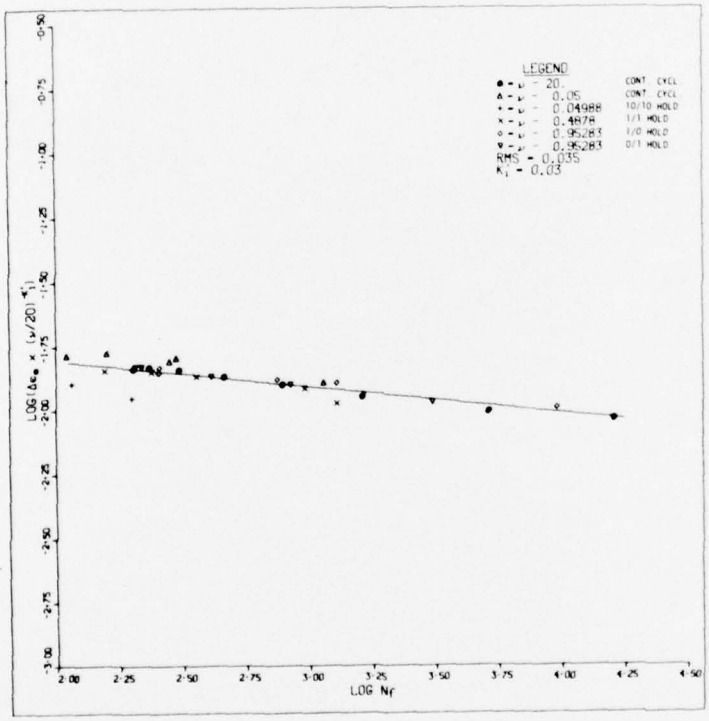

Figure 23. Plot of frequency modified elastic strain range versus cylic life from all the tests.

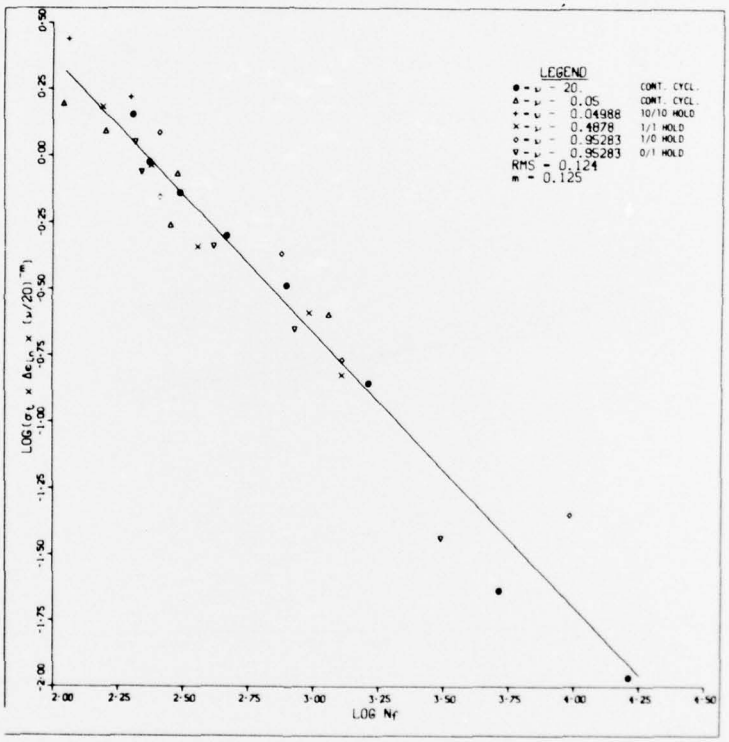

Figure 24. Plot of frequency modified damage term versus cyclic life from all tests.

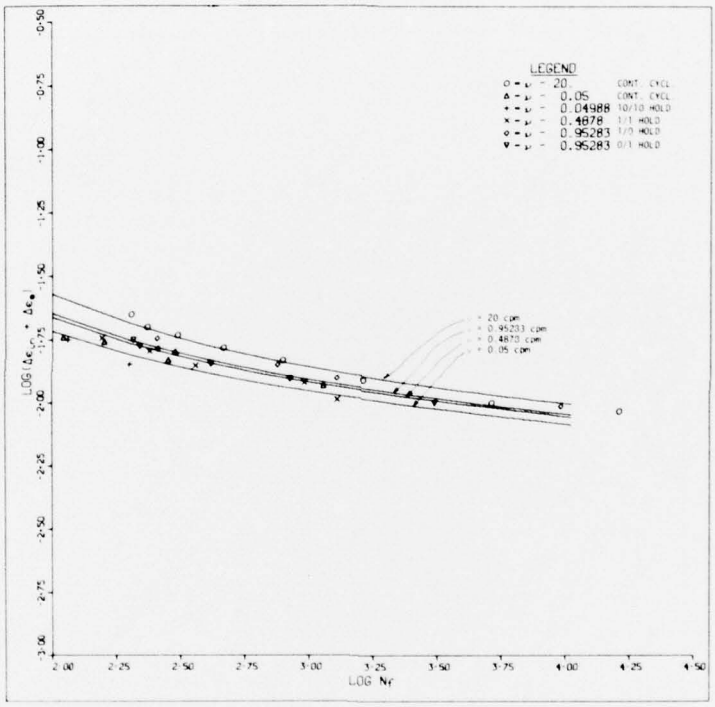

Figure 25. Plot of total strain range versus cyclic life.

☆ U. S. GOVERNMENT PRINTING OFFICE: 1977 — 757-001/279